State Key Laboratory for Diagnosis and Treatment of Infectious Diseases[1], First Affiliated Hospital, College of Medicine; Institute of Pharmacology & Toxicology[2], College of Pharmaceutical Sciences, Zhejiang University, Hangzhou, PR China

MONCPT exerts anti-cancer activities via inducing G2/M arrest and apoptosis in human bladder cancer

YUE ZHU[1,2], HAI JIANG[1], CHONG ZHANG[2], QIAO-JUN HE[2], BO YANG[1,2], LAN-JUAN LI[1], HONG ZHU[1,2]

Received May 14, 2009, accepted June 15, 2009

Hong Zhu, Institute of Pharmacology & Toxicology, College of Pharmaceutical Sciences, Zhejiang University, Hangzhou, PR China, 310058
hongzhu@zju.edu.cn
Lan-Juan Li, State Key Laboratory for Diagnosis and Treatment of Infectious Disease, First Affiliated Hospital, College of Medicine, Zhejiang University, Hangzhou, PR China, 310003
ljli@zjwst.gov.cn

Pharmazie 64: 823–828 (2009) *doi: 10.1691/ph.2009.9637*

Purpose: The potent anti-cancer capability of a novel CPT derivarate, 10-methoxy-9-nitrocamptothecin (MONCPT), has been demonstrated in our previous studies. The present study focuses on the *in vitro* and *in vivo* anti-cancer activities, the cell cycle arrest- and apoptosis-induction abilities of MONCPT on human bladder uroepithelial carcinoma 5637 cell line.
Materials and Methods: MTT assay and flow cytometric analyses were employed to evaluate the cell proliferation, cell cycle distribution and apoptosis of MONCPT-treated 5637 cells. Using 5637 xenografted nuce mice models, the *in vivo* anti-cancer capability of MONCPT were examined, as indicated by the decreased tumor volume and tumor weight. The effect of MONCPT on some of the key regulators of G2/M checkpoint and apoptosis, including CDKI-CDK-cyclin cascade, Kip1/p27 and Cip1/p21, PARP were examined using western blotting.
Results: The more potent anti-tumor activities of MONCPT than SN-38 against 5637 cells were indicated by the IC_{50} value (48 h) of 226.7 $\pm$ 0.5 nM and 2031.0 $\pm$ 0.5 nM, respectively. MONCPT treatment (0.1 μM) for 24 h caused the increment of G2/M population from 7.94% to 75.52%, indicating that MONCPT significantly triggered G2/M arrest. Moreover, MONCPT exposure (0.1 μM, 24 h) caused down-regulation of CDK7, p-Cdc2, and cyclinB1. Treatment with MONCPT (0.1 μM) for 48 h obviously induced apoptosis of 5637 cells, which was revealed by the accumulation of Annexin V-positive cells. The superior anti-tumor capabilities of MONCPT were further demonstrated in the human 5637 xenograft-bearing mice model. The administration of MONCPT at the dosages of 5, 10, 20 mg/kg for 15 days significantly inhibited the tumor growth with the inhibition rates of 64.8%, 86.2% and 96.5%, respectively.
Conclusion: The present study displayed the significant *in vitro* anti-proliferative abilities of MONCPT on human ladder cancer 5637 cells, and *in vivo* tumor-inhibitory activities on xenograft models. In addition, MONCPT was demonstrated to induce G2/M arrest and apoptosis in 5637 cells. Our findings provide evidences for the anti-tumor activity of MONCPT in the ongoing preclinical assessment.

1. Introduction

Bladder cancer is one of the most common malignancies worldwide, and more than 90% of malignant bladder cancer are transitional cell carcinomas (Raghavan 2003). Nowadays, the most efficient strategy to treat bladder cancer is surgery, and some reports indicated that the pre-surgical chemotherapy may improve the survival in bladder cancer.
Camptothecin, an alkaloid originally isolated from *Camptotheca acuminata* by Wall et al. (1966), is one of the most important lead compounds in chemotherapy. As a topoisomerase I inhibitor, CPT results in cell death by collision with replication forks and subsequent DNA damage (Tsao et al. 1993). In recent years, various CPT derivatives have been synthesized, in order to improve the anticancer potential and increase water solubility without opening the lactone E-ring. Several studies have shown that the lipophilicity confers improved cytotoxicity and topoisomerase I-inhibition onto 7,9,10-substituted camptothecin (Cesare et al. 2001; Huang et al. 2007). Among these derivatives, 10-methoxy-9-nitro-camptothecin (MONCPT, Fig. 1) has been demonstrated to exhibit potent anticancer capabilities both *in vitro* and *in vivo* against human hepatocellular carcinoma, breast cancer, non-small cell lung cancer, and androgen-independent prostate cancer (Wani 1986).
In this article, we mainly focused on the anticancer activities of MONCPT on bladder cancer, which has not been reported responding to this compound, using 5637 cell line and the corresponding nude mice xenografted models, aiming to extend our

Table 1: Effect of test compounds on experimental animals

Groups	No. of Animals		Body Weight (g)		Tumor Weight (g)	Inhibition rate (%)	Mean RTV	T/C (100%)
	Start	End	Start	End				
Control	12	12	21 ± 1	31 ± 3	1.83 ± 0.30	/	977.8	/
Irinotican 10.0 mg/kg	6	6	21 ± 1	30 ± 5	0.36 ± 0.09**	81.1	136.8	14.0
MONCPT 5.0 mg/kg	6	6	20 ± 1	29 ± 4	0.63 ± 0.12**	64.8	256.7	26.3
MONCPT 10.0 mg/kg	6	6	21 ± 1	30 ± 4	0.24 ± 0.06**	86.2	117.95	12.1
MONCPT 20.0 mg/kg	6	6	20 ± 2	32 ± 3	0.06 ± 0.03**	96.5	102.3	10.5

NOTE: The nude mice with 5637 transplant tumor were injected with (i. m.) for every 2 days for 16 days. mice were seperated to 5 groups, all alive after injection for 16 days. the criteria for therapeutic activity is: optimal growth inhibition <10 (optimal); optimal growth inhibition <25 (good); and optimal growth inhibition <50 (moderate)
$P < 0.05$
* $P < 0.001$
** $P < 0.01$

knowledge about this compound and favoring its development as a anti-tumor drug candidate (Luo 2006).

2. Investigations and results

2.1. MONCPT inhibits the proliferation of 5637 human uroepithelial bladder carcinoma cells

Both MONCPT and SN38 displayed potent cytotoxicity in a dose-dependent manner in 5637 cells (Fig. 1). The average IC_{50} values of MONCPT and SN38 against the tested cells were 226.7 ± 0.5 nM and 2031.0 ± 0.5 nM, respectively. Thus against 5637 cells, MONCPT exhibited more potent anti-proliferative activity than SN38, which was consistent with our previous results, indicating the higher efficiency of MONCPT than SN38.

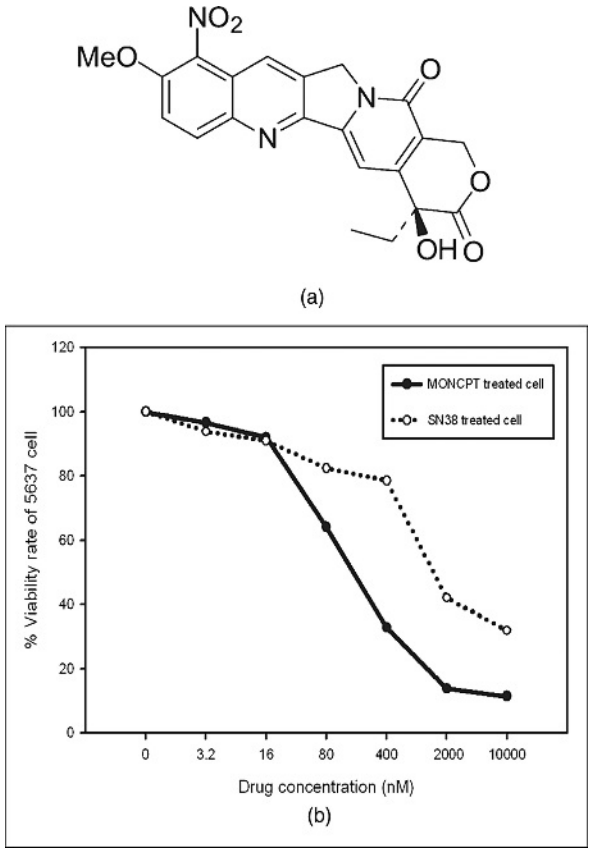

Fig. 1: Chemical structure of 10-methoxy-9-nitrocamptothecin (MONCPT) and its *in vitro* anti-proliferative activity. (A) Chemical structure of MONCPT. (B) Anti-proliferative activities of MONCPT and SN38 on 5637 human uroepithelial bladder carcinoma cells accessed by the MTT assay. 5637 cells were exposed with serials concentration of MONCPT or SN38 for 72 h. The black line refers to the MONCPT-treated cells and the dot line shows the viability rate of SN38-treated cells. ($p < 0.05 - 0.001$)

2.2. MONCPT exerts significant anti-tumor activity against nude mice 5637 xenograft models

Nude mice bearing human bladder cancer 5637 were used to evaluate the effect of MONCPT and the reference compound irinotecan on tumor growth *in vivo*. As demonstrated in the Table, MONCPT produced dose-dependent tumor-growth-inhibition effects in nude mice 5637 xenograft models. The i.m. administration of MONCPT at doses of 5, 10, and 20 mg/kg for 15 days reduced 64.8%, 86.2% and 96.5% tumor growth, respectively. Irinotecan at dose of 10 mg/kg with the same schedule caused comparable potent reduction in tumor growth (81.1%) with MONCPT-treated groups. Figure 2 revealed that from day 1 to day 15, the tumor volumes in the control

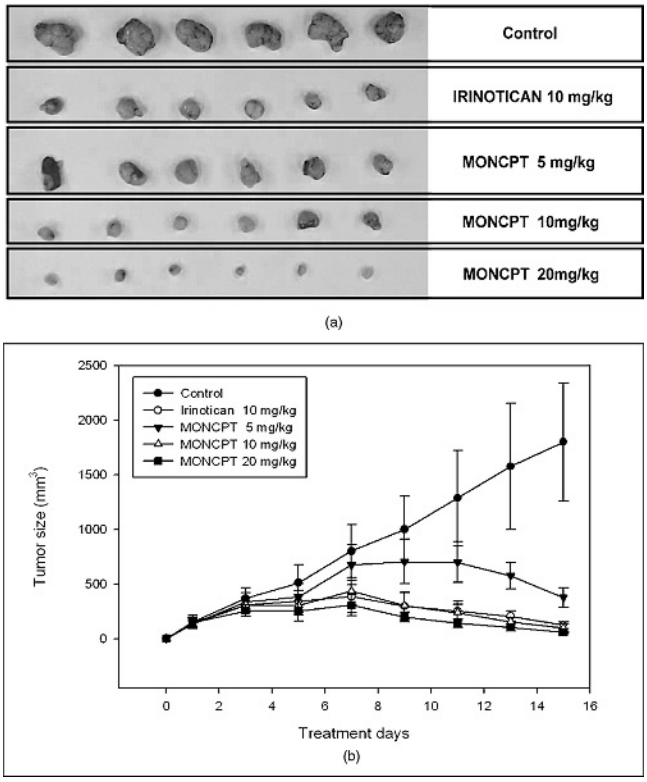

Fig. 2: Antitumor potency of MONCPT on human uroepithelial bladder cancer 5637 xenograft models. The mice transplanted with 5637 human xenograft were randomly divided into 5 groups and given injection of MONCPT (5 mg/kg, 10 mg/kg and 20 mg/kg)) or irinotican (10 mg/kg). (A) The actual tumor sizes of sacrificed mice in different groups were showed. (B) Tumor volumes of different groups were expressed as mean ± SD

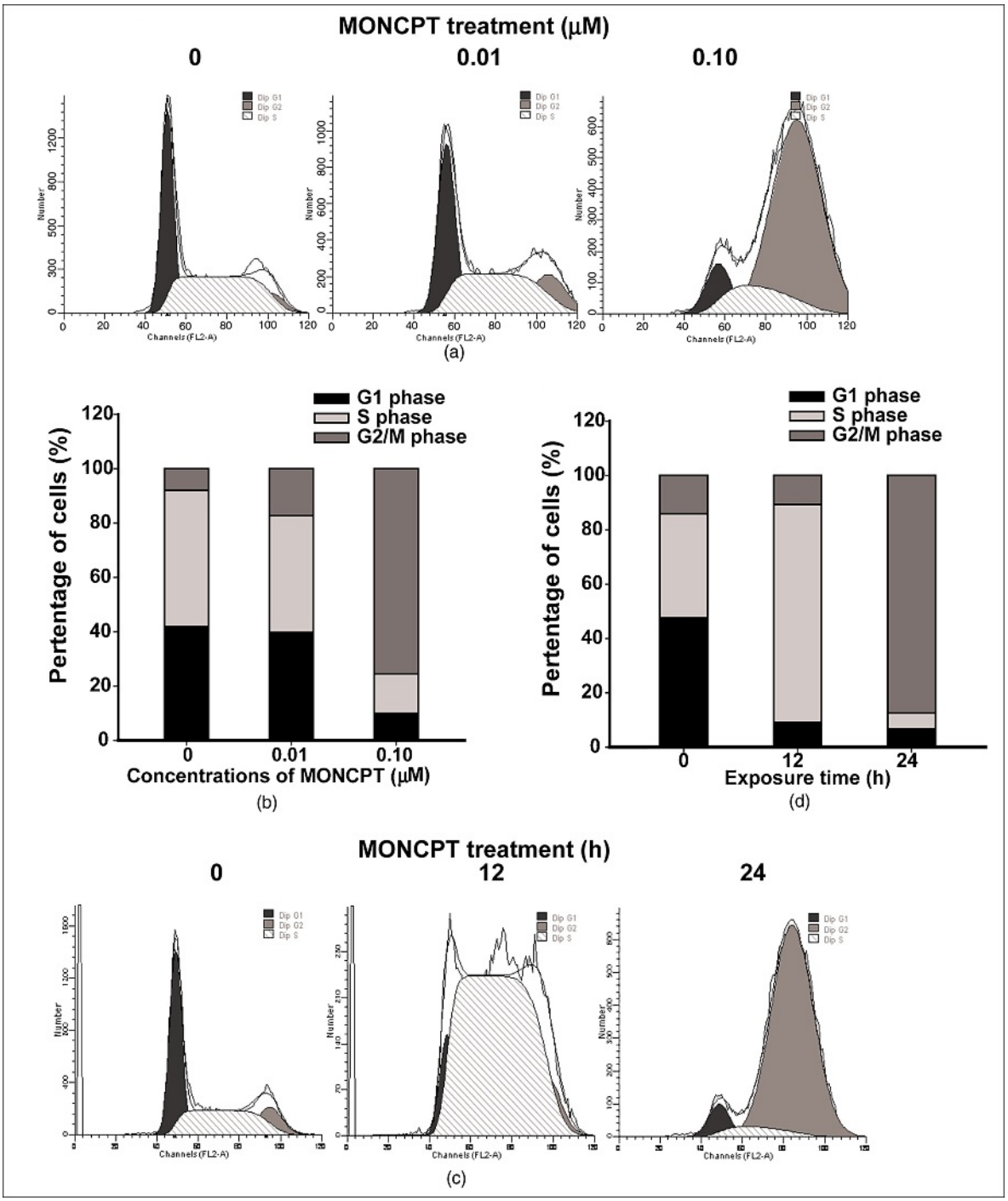

Fig. 3: MONCPT arrested 5637 cells at G2/M phase in concentration- and time-dependent manners. (A) MONCPT induced concentration-dependent G2/M arrest in 5637 cells. The cells were treated with MONCPT (0.01 μM and 0.1 μM) for 24 h. DNA content of 10,000 events was analyzed by flow cytometry. (B) The cell cycle distribution histograms were presented, indicating each proportion of cells arrested in each cell cycle phases including G1, S and G2/M phases. (C) Exposure to MONCPT caused time-dependent G2/M arrest in 5637 cells. The cells were treated with 0.1 μM MONCPT for 0 h, 12 h and 24 h, and harvested for analyses. Histograms of cell proportion (%) in each cell cycle phases of each group were presented in (D)

group achieved a 11.5-fold increase, whereas tumor volumes in MONCPT treatment groups obtained 2.7-fold (5 mg/kg), 0.7-fold (10 mg/kg) and 0.4-fold (20 mg/kg) increases, respectively; whereas in the irinotecan-treated (10 mg/kg) group, the tumor volumes achieved a 1.2-fold increase, indicating the more significant tumor-arresting activities of MONCPT than irinotecan. Additionally, T/C % was used to further evaluate the effect of MONCPT *in vivo*. The Table shows that at doses of 5 mg/kg, 10 mg/kg, 20 mg/kg, the T/C% value of MONCPT-treated groups were 26.3%, 12.1% and 10.5%; and at the same dosage, MONCPT exhibited a slight greater activity than irinotecan (10 mg/kg, T/C: 14.0%).

Collectively, the superior anti-tumor efficiency possessed by MONCPT was stronger than, or at least comparable with irinotecan, a widely-used CPT derivative. Together with the little effect on the mice body weight (Table 1), these data provide further evidence for the possible development of MONCPT.

2.3. MONCPT induces G2/M arrest of 5637 cells

Flow cytometric analysis was performed to determine whether MONCPT-inhibited proliferation was due to the cell cycle arrest. Our data shows that 24 h treatment of MONCPT remarkably caused concentration-dependent G2/M arrest of 5637 cells,

as indicated by the accumulation of G2/M population, from 7.94% in control group to 75.52% in MONCPT (0.1 μM) group (Fig. 3A and 3B). In addition, Fig. 3C and 3D demonstrate that 0.1 μM MONCPT caused the accumulation of cells in the G2/M phase in a time-dependent manner. 5637 cells were incubated in 0.1 μM MONCPT for 0 h, 12 h and 24 h. The percentages of G2/M population were 9.65% (0 h), 17.08% (12 h) and 87.44% (24 h). The data showed that the G2/M arrest was triggered by MONCPT, and suggested that the cell cycle arrest may contribute to the cell growth inhibitory effects of MONCPT.

2.4. MONCPT elicited-G2/M arrest was associated with the modulation of cell cycle regulatory proteins

To investigate the mechanisms involved in MONCPT effects on cell cycle regulatory molecules, we examined the expression of cell cycle regulatory proteins in MONCPT-exposed 5637 cells using western blotting. The molecular activities associated with CDKs drive cell cycle progression through transitional checkpoints by activating CDK-cyclin complexes (Morla 1989). In our study, as shown in Fig. 4A, down-regulation of cyclin B1 and the phosphorylation of Thr161 (active site) of Cdc2 in MONCPT-exposed cells (0.1 μM, 24 h) were observed, implying the reduction of cyclin B1/Cdc2 complex activity which was responsible for the G2/M transition during cell cycle progression. The impact of MONCPT treatment on another important complex cyclin H/CDK7 was also be tested by measuring the protein level of these two components. As shown in Fig. 4B, MONCPT imposed little effect on the protein level of CDK7 and cyclin H, suggesting that this complex was not crucial for the G2/M arrest caused by MONCPT.

These results collectively suggested that the induction of G2/M arrest in MONCPT-exposed 5637 cells were attributed to the reduction of protein level and/or activity modulation of cyclinB1/Cdc2 complex. The block of cell cycle progression in G2/M transition allow DNA repair before commitment into M phase in MONCPT-treated cells, and also may assist the inhibition of cell proliferation represented in our above-mentioned data.

2.5. MONCPT upregulates CDKIs Cip1/p21 and Kip1/p27 protein expression in 5637 cells

Generally, induction of p21 or p27 expression inhibits the activities of CDK2 and arrests cells at the G1/S transition of the cell cycle progression (Harper 1993). Increasing of p21 has been reported to be regulated by either a p53-dependent or p53-independent mechanism (Kay 2008). Recently, it was reported that p21 induced an additional block at the G2 phase and inhibited cell entry into the M phase in a p53-independent mechanism. The 5637 cell line susceptible to the MONCPT treatment was previously reported as a mutant-p53-possessing cell line, owing to an in-frame deletion of tyrosine126 (Cooper 1994). As shown in Fig. 4C, upon the treatment of MONCPT, p21 and p27 were time-dependently up-regulated in 5637 cells, demonstrating the involvement of p53-independent regulation of p21 and p27.

2.6. MONCPT causes apoptosis in 5637 cells

Most CPT derivatives kill tumor cells via inducing apoptosis of these malignant cells. In our study, the 5637 cells treated with 0.1 μM MONCPT for 24 h and 48 h displayed morphologic changes including membrane blebbing and detachment from the surface of the flask (Fig. 5B). Then we used Annexin V-PI double staining and flow cytmetric analysis to quantify apoptotic cells. Apoptosis, as measured by flow cytometry, was

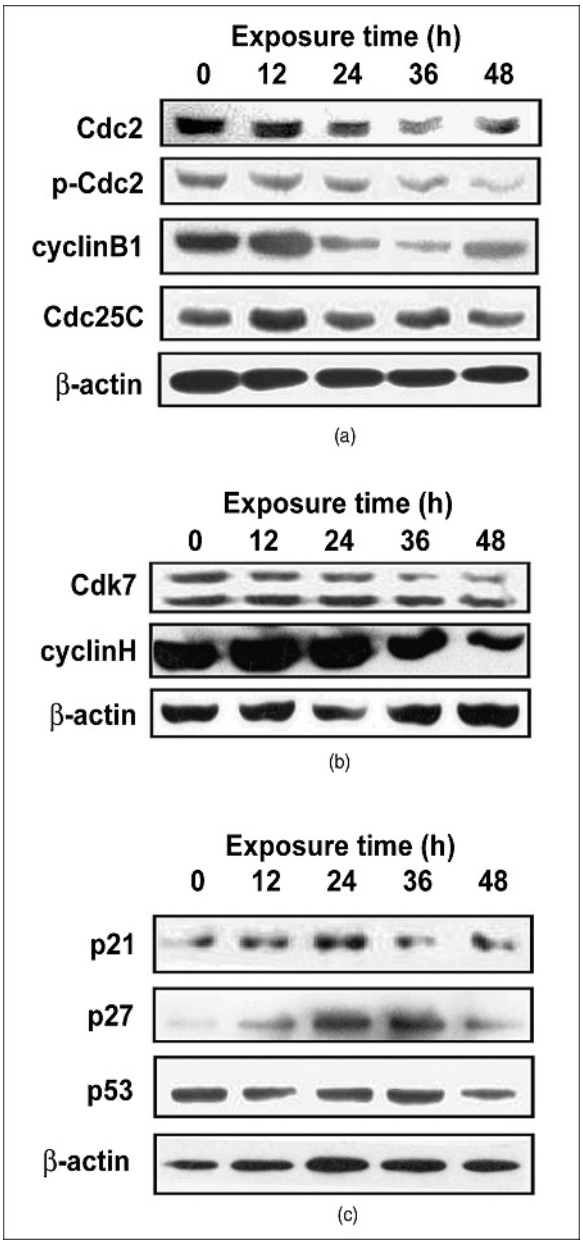

Fig. 4: Effects of MONCPT on G2/M cell cycle regulators. 5637 cells were treated with MONCPT (0.1 μM) for 0, 12 or 24 h, harvested, lysed and analyzed using western blotting. Equal amounts (40 μg/lane) of cellular protein were fractionated. (A) MONCPT exposure down-regulated the protein level of cdc2, p-cdc2 (Thr 161) and cyclinB1 in 5637 cells. (B) MONCPT decreased the protein level of CDK7 and cyclinH of 5637 cells. (C) The protein levels of p21 and p27 were affected by MOMCPT treatment

represented as the percentage of cells that stained positive for annexin V. Fig. 5A showed that MONCPT treatment (0.1 μM) led to significant apoptosis of 5637 cells in a time-dependent manner, with 29.3% and 35.2% in 24 h- and 48 h-treated cells, respectively. We further examined the PARP cleavage, a well-accepted marker of irreversible apoptosis using western blotting. As demonstrated in Fig. 5C, full-length PARP was cleaved time-dependently upon the treatment of MONCPT, denoting the undergoing of apoptosis.

3. Discussion

Camptothecin and its various derivatives have been reported to possess potent anti-tumor activity via inhibiting topoisomerase I and subsequent DNA damages. Our research focused on the screening and exploring of the novel camptothecin ana-

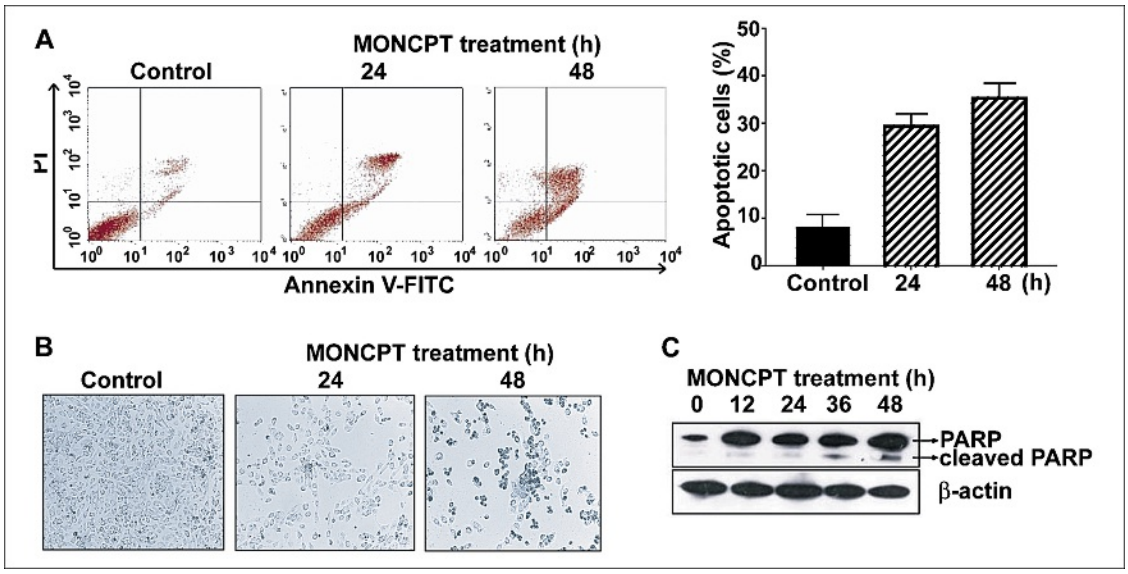

Fig. 5: MONCPT triggers apoptosis of 5637 cells. MONCPT (0.1 μM) induced apoptosis of 5637 cells in a time-dependent manner. (A) Annexin V-PI staining was used to evaluate the apoptosis. Cells were exposed to MONCPT (0.1 μM) for 24 h or 48 h. The Annexin V positive cells were defined as apoptotic cells. Total number of events analyzed for each sample was 30 000. Three independent experiments were taken and the apoptotic rates were expressed as mean ± SD (n = 3). (B) The morphologic change of 5637 cells treated with MONCPT (0.1 μM) was observed. (C) MONCPT exposure (0.1 μM) caused PAPR cleavage, denoting the undergoing of apoptosis

logues, and elucidating the underlying anti-cancer mechanisms. In our previous studies, MONCPT stood out by its improved anti-tumor activity both *in vitro* and *in vivo*, and well-defined topo I inhibiting mechanisms, as comparable with SN38 (Luo 2006). MONCPT inhibited cell proliferation in various cancer cell lines, but its effect on bladder cancer has not been reported. Therefore, the present study chose the bladder cancer 5637 cell line to investigate the anti-cancer efficiency of MONCPT, in order to extend our knowledge about this compound.

According to our previous study, the IC_{50} values of MONCPT for five of nine tested cancer cell lines were lower than those of SN38, indicating that MONCPT possessed higher anti-proliferative activities in certain cancer species, such as A549 and PC3 cancer cell lines (Luo 2006). In this study, we firstly examined the 5637 cell proliferation upon the treatment of MONCPT and SN38, respectively. The data achieved using MTT assay (Fig. 1B) demonstrated that MONCPT exhibited more significant anti-proliferative activities against 5637 cells than SN38, with a much lower IC_{50} value of 226.7 ± 0.5 nM (SN38: 2031.0 ± 0.5 nM). Furthermore, in the 5637 xenografted nude mice models, we showed that MONCPT exerted stronger *in vivo* anti-tumor activity than irinotecan. As displayed in Table 1 and Fig. 2, the tumor volumes were distinctly diminished, and the tumor inhibition rates were 64.8%, 86.2% and 96.5% at day 15 without evident loss of body weight in 5 mg/kg, 10 mg/kg and 20 mg/kg MONCPT-treated groups, respectively. Irinotecan was injected at the dose of 10 mg/kg, and achieved 81.1% tumor-inhibition which was less than the equivalent-dosage-MONCPT-treated groups. Taken together, both *in vitro* and *in vivo* models supported the notion that against the human bladder cancer 5637, MONCPT possessed better anti-tumor activities comparing with the widely-used CPT derivative irinotecan.

Studies have shown correlations between deregulated cell cycle progression and cancer proliferation, suggesting that cell cycle inhibition could be an important target for the management of cancer (Jacks 1996). Multiple regulators are responsible for coordinating advancement through each phase of the cell cycle progression. Among these regulators and key events, the sequential activation of cyclin-CDK complexes (cyclin-dependent kinases, CDKs), which are in turn regulated by positive (cyclins) and negative (CDK inhibitory proteins) effectors, play the ultimate role in cell cycle progression control and modulation. The cyclin B/Cdc2 complex directs the entry and exit from cell mitosis, which regulates cell progression from G2 phase to M phase. The inactive cyclin B/Cdc2 complex accumulates during G2 phase until it is activated by the dephosphorylation of Thr-14 and Tyr-15 by CDC25 phosphatase, which promotes entry into mitosis. In the current study, on the basis of validated G2/M arrest induced by MONCPT (Fig. 3), our data showed both the decreased protein levels of cyclinB1 and Cdc2, as well as the reduced phosphorylation level of the active site (Thr 161) of Cdc2 were triggered by the MONCPT exposure to 5637 cells (Fig. 4A), suggesting the loss of cyclinB/Cdc2 complex activity may eventually lead to the G2/M transition block.

Recently, more and more attention is focused on drugs which can induce growth inhibitory effects even in the late stages of therapy. As an important part of the DNA repair system, cell cycle checkpoints are responsible for ensuring the orderly and timely progression of some critical events such as DNA replication and chromosome segregation in cells. In response to DNA DSBs, cell cycle checkpoints are activated to arrest cells at G1/S, S, or G2/M transitions points, allowing time for the cells to repair the damage or, in the case of unrepairable lesions, to execute apoptosis. Therefore, not all the arrested cancer cells would undergo apoptosis, if they get the chance to repair their damaged DNA. The recovery from the DNA damage imposed by chemotherapeutic agents is one of the major reasons for the resistances of cancer cells to chemotherapy. Accordingly, to eliminate cancer cells more effectively, the better strategy for the anti-tumor drug candidates is to trigger apoptosis in cancer cells (Gastman 2000; Gurumurthy et al. 2001). In this perspective, we incubated 5637 cells with 0.1 μM MONCPT for 48 h, and found that over 35% of the cells were undergoing apoptosis, revealed by the Annexin V-positive staining and the cleavage of PARP. Thus, upon 24 h incubation, 87.4% of the 5637 cells exposed to 0.1 μM MONCPT were blocked at the G2/M transition, while after another 24 h, 35.2% of the treated cells would execute apoptosis.

In summary, the present study demonstrates that MONCPT is capable of inhibiting the proliferation of human bladder cancer 5637 cells *in vitro*, and arresting the growth of 5637 xenografted tumors *in vivo*, possibly via inducing G2/M arrest and triggering the subsequent apoptosis. These results collectively provide new data for the anti-tumor capability of MONCPT as a drug candidate for treating bladder cancer.

4. Experimental

4.1. Chemical compound

MONCPT was produced according to Wani's method (Wani et al. 1987). SN38 and irinotecan were purchased from HengRui Medicine, Inc. Lian Yungang, Jiangsu China. Both compounds were dissolved at 10 mM in DMSO and diluted with HG-DMEM (Life Technologies) as stock solutions for *in vitro* studies. For the *in vivo* test, MONCPT was dissolved and diluted in injectable oleum camelliae before being administrated to xenografted nude mice. Irinotecan was dissolved in sodium chloride before injection.

4.2. Cell culture

The human uroepithelial bladder carcinoma cell line, 5637, was obtained from the the cell bank of the Shanghai Institute of Materia Medica, Chinese Academy of Sciences. The cells were maintained in HG-DMEM (4.5 g/L glucose), supplemented with 10% fetal calf serum (Life Technologies), L-glutamine (2 mmol/L), penicillin (100 IU/mL), streptomycin (100 Ag/mL), and HEPES (10 mmol/L, pH 7.4), incubated in an atmosphere of 20% O_2 air, 5% CO_2 at 37 °C. Cells were subcultured every other day with trypsin/EDTA solution (saline containing 0.05% trypsin, 0.01 M sodium phosphate (pH 7.4) and 0.02% EDTA).

4.3. Cytotoxicity assay

Human uroepithelial bladder cancer 5637 cells were seeded at 2×10^3 per well in 96-well culture plates and incubated overnight with HG-DMEM containing 10%FBS overnight, then treated in triplicate with serial concentrations of MONCPT or SN38 for 48 h. Afterwards, cells were incubated with 3-(4,5-dimethylthiazol-2-yl)-2,5- diphenyltetrazolium bromide (MTT, 5 mg/ml, 20 μl/well), and the generated colored product in the cells was dissolved in DMSO and was measured at 570 nm using a multiskan spectrum (Thermo Electron Co., Vantaa, Finland). The inhibition rate on cell proliferation was calculated for each well as (A570 control cells - A570 treated cells) / A570 control cells × 100%. The IC50 values were determined by Logit.

4.4. Antitumor activity against of 5637 xenograft in nude mice

The xenograft model of uroepithelial bladder carcinoma cell was established subcutaneously by injecting 8×10^6 5637 cells to 4- to 5-week-old BALB/c female athymic nude mice (National Rodent Laboratory Animal Resource, Shanghai, China). Treatments were initiated when tumors reached a mean group size of about 150 mm^3, and the mice were randomly assigned to 5 groups as follows: control, irinotican 10.0 mg/kg, MONCPT 5.0 mg/kg, MONCPT 10.0 mg/kg, MONCPT 20.0 mg/kg. MONCPT (5, 10, and 20 mg/kg) was formulated in injectable oleum camelliae and administered i.m. once every 2 days for 15 days. Tumor size was measured by calipers (length and width) every 2 days. Tumor volumes were determined by $V = 1/2$ (length × width^2). The individual relative tumor volume (RTV) was calculated as follows: $RTV = TVn/TV_0$, where TVn is the tumor volume at day n, and TV_0 is the tumor volume at day 0. The therapeutic effect of compounds was expressed in terms of T/C % (mean RTV of the treated group/mean RTV of the control group × 100%).

4.5. Cell cycle and apoptosis analysis

Cells (5×10^6) in 6 well plates were treated with 0.1 μM of MONCPT for 48 h, then harvested and washed with PBS for 3 times and fixed with 70% ethanol at 4 °C for 1 h and then washed with PBS again. The pellet was suspended in RNaseA solution (20 μg/ml), incubated at 37 °C for 15 min and stained with propidium iodide (PI, Sigma) for 30 min in the dark at room temperature. The cellular DNA content was analyzed on a FACS Calibur flow cytometer using the Cell Quest Pro software (BD Biosciences, San Jose, CA). The percentage of each population was measured using Mod FIT software (BD Biosciences). Apoptosis was assessed using annexin V (BD Biosciences-Pharmingen) and propidium iodide (PI, BD) staining. Cells staining positive for annexin V were scored as apoptotic. At least 30 000 cells were analyzed for each data point.

4.6. Western blotting

Collected cells (1×10^6/sample) were resuspended with lysis buffer (50 mM Tris-HCl, pH 7.4, 150 mM NaCl, 0.5% Nonidet P-40, 50 mM NaF, 1 mM Na_3VO_4, 1 mM phenylmethylsulfonyl fluoride, 25 μg/ml leupeptin, and 25 μg/ml aprotinin) and sonicated at 4 °C. Samples were subjected to SDS-PAGE on 10 or 15% gel and separated proteins were transferred onto PVDF membrane (Pierce Biotechnology, Inc., Rockford, IL). Membranes were blocked with 5% BSA for 1 h at room temperature, and, as desired, probed with primary antibodies, including Cip1/p21, Kip1/p27, CDK7, cyclin H, cleaved PARP, Cdc2, cyclin B1 and β-actin overnight at 4 °C followed by peroxidase-conjugated appropriate secondary antibody (all antibodies are from Santa Cruz Biotechnology, Inc., Santa Cruz, CA) and ECL detection.

Acknowledgements: This study was financially supported by Grants from Natural Science Foundation of China (30801406) to Hong Zhu, Zhejiang Provincial Foundation of Natural Science (R2080326) to Qiao-Jun He, Zhejiang Provincial Program for the cultivation of High-level Innovative Health talents and the Foundation of high-tech talents of Cao guangbiao to Bo Yang.

References

Cesare M, Pratesi G, Perego P, Carenini N, Tinelli S, Merlini L, Penco S, Pisano C, Bucci F, Vesci L, Pace S, Capocasa F, Carminati P, Zunino F (2001) Potent antitumor activity and improved pharmacological profile of ST1481, a novel 7-substituted camptothecin. Cancer Res 61: 7189–7195.

Cooper MJ, Haluschak JJ, Johnson D, Schwartz S, Morrison LJ, Lippa M, Hatzivassiliou G, Tan J (1994) p53 Mutations in bladder carcinoma cell lines. Oncol Res 6: 569–579.

Gastman BR (2000) Apoptosis and its clinical impact. Head Neck 123: 409–425.

Gurumurthy S, Vasudevan KM, Rangnekar VM (2001) Regulation of apoptosis in prostate cancer. Cancer Metastasis Rev 20: 225–243.

Harper JW, Adami GR, Wei N, Keyomarsi K, Elledge, SJ (1993) The p21 Cdk-interacting proteinCip1 is a potent inhibitor of G1 cyclin-dependent kinases. Cell 75: 805–816.

Huang M, Gao HY, Chen Y, Zhu H Cai Y, Zhang X, Miao Z, Jiang H, Zhang J, Shen H, Lin L, Lu W, Ding J (2007) Chimmitecan, a novel 9-substituted camptothecin, with improved anticancer pharmacologic profiles in vitro and in vivo. Clin Cancer Res 13: 1298–1307.

Jacks T, Weinberg RA (1996) Cell-cycle control and its watchman. Nature 381: 643–644.

Kay FM, Nicole S, Greg H, et al. (2008) p53-Dependent and independent expression of p21 during cell growth, differentiation, and DNA damage. Genes Developm 9: 935–944.

Luo PH, He QJ, Yang B, Hu Y, Lu W, Cheng Y, Yang B (2006) Potent antitumor activity of 10-methoxy-9-nitrocamptothecin. Mol Cancer Ther 5: 962–968.

Raghavan D (2003) Molecular targeting and pharmacogenomics in the management of advanced bladder cancer. Cancer 97: 2083–2089.

Tsao YP, Russo A, Nyamuswa G, Sibler R, Liu LF (1993) Interaction between replication fork and topoisomerase I-DNA cleavable complexes. Study in cell-free SV40 DNA replication system. Cancer Res 53:1–8.

Wall ME, Wani MC, Cook CE, Palmer KH, McPhail AT, Sim GA (1966) Plant antitumor agents, the isolation and structure of camptothecin, a novel alkaloidal leukemia and tumor inhibitor from Camptotheca acuminates. J Am Chem Soc 88: 3888–3890.

Wani MC, Nicholas AW, Wall ME (1986) Plant antitumor agents. 23. Synthesis and antileukemic activity of camptothecin analogues. J Med Chem 29:2858–2863.

Wani MC, Nicholas AW, Wall ME (1987) Plant antitumor agents. 28. Resolution of a key tricyclic synthon, 5′(RS)-1,5-dioxo-5′-ethyl-5′-hydroxy-2′H,5′H,6′H-6′-oxopyrano[3′, 4′-delta 6,8-tetrahydro-indolizine: total synthesis and antitumor activity of 20(S)- and 20(R)-camptothecin. J Med Chem. 30: 2317–2319.

Morla A, Draetta G, Beach D, Wang JY (1989) Reversible tyrosine phosphorylation of Cdc2: dephosphorylation accompanies activation during entry into mitosis. Cell 58: 193–203.